Zbtb7b engages the long noncoding RNA Blnc1 to drive brown and beige fat development and thermogenesis

Siming Li[a,b,1], Lin Mi[a,b], Lei Yu[a,b], Qi Yu[a,b], Tongyu Liu[a,b], Guo-Xiao Wang[a,b], Xu-Yun Zhao[a,b], Jun Wu[a,c], and Jiandie D. Lin[a,b,1]

[a]Life Sciences Institute, University of Michigan, Ann Arbor, MI 48109; [b]Department of Cell & Developmental Biology, University of Michigan Medical Center, Ann Arbor, MI 48109; and [c]Department of Molecular & Integrated Physiology, University of Michigan Medical Center, Ann Arbor, MI 48109

Edited by Steven A. Kliewer, The University of Texas Southwestern Medical Center, Dallas, TX, and approved July 12, 2017 (received for review March 1, 2017)

Brown and beige adipocytes convert chemical energy into heat through uncoupled respiration to defend against cold stress. Beyond thermogenesis, brown and beige fats engage other metabolic tissues via secreted factors to influence systemic energy metabolism. How the protein and long noncoding RNA (lncRNA) regulatory networks act in concert to regulate key aspects of thermogenic adipocyte biology remains largely unknown. Here we developed a genome-wide functional screen to interrogate the transcription factors and cofactors in thermogenic gene activation and identified zinc finger and BTB domain-containing 7b (Zbtb7b) as a potent driver of brown fat development and thermogenesis and cold-induced beige fat formation. Zbtb7b is required for activation of the thermogenic gene program in brown and beige adipocytes. Genetic ablation of Zbtb7b impaired cold-induced transcriptional remodeling in brown fat, rendering mice sensitive to cold temperature, and diminished browning of inguinal white fat. Proteomic analysis revealed a mechanistic link between Zbtb7b and the lncRNA regulatory pathway through which Zbtb7b recruits the brown fat lncRNA 1 (Blnc1)/heterogeneous nuclear ribonucleoprotein U (hnRNPU) ribonucleoprotein complex to activate thermogenic gene expression in adipocytes. These findings illustrate the emerging concept of a protein–lncRNA regulatory network in the control of adipose tissue biology and energy metabolism.

brown fat | beige fat | Zbtb7b | Blnc1 | lncRNA

Brown fat contains abundant mitochondria that dissipate energy to generate heat via uncoupling protein 1 (UCP1) (1–5). Brown fat thermogenesis is important for maintaining body temperature during cold stress and contributes to energy balance. Genetic ablation of UCP1$^+$ adipocytes rendered mice cold sensitive and prone to diet-induced obesity (6), whereas genetic and pharmacological activation of brown fat thermogenesis resulted in increased energy expenditure, reduced adiposity, and improved glucose and lipid homeostasis (7–10). Beyond UCP1-mediated thermogenesis, brown adipose tissue (BAT) also engages a parallel mechanism to regulate metabolic functions of other tissues through its secretion of endocrine factors (11, 12), such as Neuregulin 4 (Nrg4) (13). Nrg4 preserves metabolic homeostasis during diet-induced obesity through modulating de novo lipogenesis in the liver, a mechanism that is independent of brown fat thermogenesis. As such, it is conceivable that activation of brown fat thermogenesis (3, 14, 15) and/or modulation of its endocrine function (11, 12) may hold the promise of developing novel therapies targeting metabolic diseases.

The discovery of brown fat in adult humans (16–19) marked a turning point in understanding the role of brown fat thermogenesis in human physiology and disease. Human brown fat contains the classical brown adipocytes and a distinct class of brown-like adipocytes, termed "beige/brite adipocytes," that share considerable molecular and metabolic characteristics (5). In rodents, brown and beige adipocytes originate from distinct lineages during development. The former shares a common progenitor lineage with skeletal myocytes (20), whereas the latter appears to derive from multiple progenitors in the s.c. fat in response to browning stimuli (21–23). A number of transcription factors and cofactors have been identified that regulate the determination, differentiation, maturation, and maintenance of thermogenic adipocytes (3, 24). Among these, Prdm16 and EBF2 are emerging as key factors that stimulate thermogenic gene programs during brown and beige adipocyte differentiation. Interestingly, while Prdm16 is largely dispensable for brown fat development, it is required for cold-induced browning of s.c. fat and maintaining the thermogenic capacity of brown fat during aging (25, 26). Recent studies have demonstrated that IFN regulatory factor-4 (IRF4) and zinc-finger protein 516 (ZFP516) are inducible activators of brown and beige adipocyte differentiation and function (27, 28). These transcription factors recruit additional chromatin-remodeling proteins, such as PPARγ coactivator-1α (PGC-1α) and euchromatic histone-lysine *N*-methyltransferase 1 (EHMT1) (29, 30), to drive transcriptional activation of genes underlying fuel oxidation and thermogenesis. Despite this, the nature of the transcriptional network that governs various aspects of brown and beige fat biology remains incompletely defined. Further, how this protein regulatory network interfaces with long noncoding RNAs (lncRNAs), an emerging class of developmental regulators, remains largely unexplored.

The term "lncRNAs" commonly refers to RNA transcripts that are longer than 200 nt but lack protein-coding potential (31, 32). The expression of lncRNAs exhibits a high degree of tissue specificity and developmental regulation, underscoring their potential to function as regulatory switches. LncRNAs have been

Significance

Brown and beige fat function has important implications for metabolic physiology and the treatment of metabolic disorders. How transcription factors interface with long noncoding RNAs (lncRNAs), an emerging class of regulatory factors, to drive development and thermogenesis of brown/beige fat remains essentially unknown. Here we identified Zbtb7b as an activator of the thermogenic gene program through a genome-wide functional screen and showed that it plays an essential role in cold-induced thermogenesis and beige fat formation. Mechanistically, Zbtb7b forms a ribonucleoprotein transcriptional complex with the lncRNA Blnc1 and drives thermogenic gene expression via a feedforward loop. This work illustrates the emerging concept of a protein–lncRNA regulatory network in the control of adipose tissue biology and energy metabolism.

Author contributions: S.L., L.M., and J.D.L. designed research; S.L., L.M., L.Y., Q.Y., T.L., and X.Y.Z. performed research; G.X.W. and J.W. contributed new reagents/analytic tools; S.L., L.M., X.Y.Z., and J.D.L. analyzed data; and S.L. and J.D.L. wrote the paper.

The authors declare no conflict of interest.

This article is a PNAS Direct Submission.

Data deposition: The microarray dataset described in this paper has been submitted to the National Center for Biotechnology Information Gene Expression Omnibus (GEO) database, https://www.ncbi.nlm.nih.gov/geo/ (accession no. GSE100924).

[1]To whom correspondence may be addressed. Email: simingli@umich.edu or jdlin@umich.edu.

This article contains supporting information online at www.pnas.org/lookup/suppl/doi:10.1073/pnas.1703494114/-/DCSupplemental.

shown to play an important role in the regulation of diverse biological processes, including transcriptional regulation, cell differentiation, tissue development, and tumorigenesis and metastasis. Several lncRNAs have been identified that regulate hepatic lipid metabolism (33, 34), pancreatic development (35, 36), and adipocyte differentiation (37–40). We previously discovered brown fat lncRNA 1 (Blnc1) as an inducible lncRNA that promotes brown and beige adipogenesis through its interaction with EBF2 (39). Blnc1 is highly conserved at the sequence and functional levels between mice and humans. More recently, lnc-BATE1 was identified as another lncRNA regulator of brown adipocyte differentiation through adipocyte transcriptome analysis (37). Interestingly, both Blnc1 and lnc-BATE1 physically associate with the RNA-binding protein hnRNPU to regulate adipocyte gene expression (37, 41).

In this study, we developed a genome-wide functional screen to interrogate the transcriptional regulatory network that activates thermogenic gene program in brown and beige adipocytes. Our work identified the transcription factor zinc finger and BTB domain-containing 7b (Zbtb7b) as a regulator of brown and beige fat development and thermogenesis that acts by recruiting the Blnc1/hnRNPU ribonucleoprotein transcriptional complex. Our findings illustrate the emerging concept of a protein–lncRNA regulatory network in the control of adipose tissue biology and energy metabolism.

Results

Interrogation of the Transcriptional Network That Drives the Thermogenic Adipocyte Gene Program. A central aspect of brown and beige adipogenesis is the transcriptional activation of genes underlying mitochondrial fuel oxidation and thermogenesis. Previous studies have identified several transcription factors and cofactors that regulate the determination, differentiation, maturation, and maintenance of thermogenic fat cells (3, 24). Despite this, the nature of the transcriptional network that governs the development and function of brown and beige adipocytes remains elusive. To address this, we developed a genome-wide screen to functionally interrogate the transcription factors and cofactors for their ability to drive thermogenic adipocyte differentiation. We have previously constructed a Transcription Factor ORF Collection (TFORC) that contains ≈1,510 individual ORFs encoding human transcription factors or cofactors (42). The TFORC covers ≈56% of all predicted transcription factors and cofactors in the human genome. Using high-throughput Gateway cloning, we constructed retroviral vector pools containing four individual factors, transduced C3H10T1/2 (10T1/2) mesenchymal progenitor cells, and subjected them to the brown

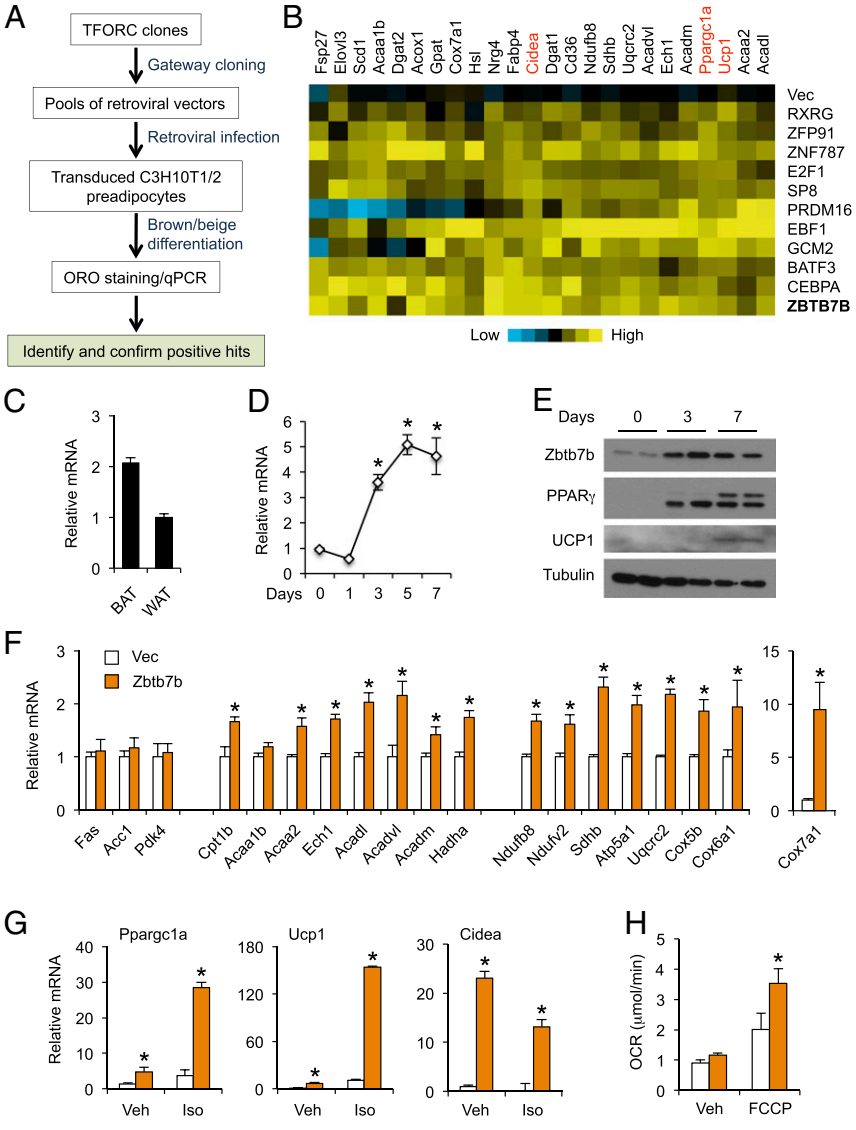

Fig. 1. Identification of Zbtb7b as an inducer of thermogenic adipocyte differentiation. (*A*) Functional screen of transcription factors and cofactors that promote thermogenic adipocyte gene expression and differentiation. ORO, Oil Red O staining. (*B*) Heat map representation of the effects of individual factors on mitochondrial and thermogenic gene expression in differentiated 10T1/2 adipocytes. (*C*) qPCR analysis of Zbtb7b expression in BAT and WAT. Data represent mean ± SEM. (*D*) qPCR analysis of Zbtb7b expression during brown adipocyte differentiation. Data represent mean ± SD. $*P < 0.01$, vs. d 0. (*E*) Immunoblots of brown adipocyte lysates during differentiation. (*F*) qPCR analyses of gene expression in differentiated 10T1/2 adipocytes transduced with vector (open bars) or ZBTB7B retrovirus (red bars). (*G*) qPCR analyses of gene expression in 10T1/2 adipocytes treated with vehicle (Veh) or isoproterenol (Iso) for 5 h. (*H*) Oxygen consumption rate (OCR) in transduced 10T1/2 adipocytes. Data in *F*–*H* represent mean ± SD. $*P < 0.05$, Zbtb7b vs. vector; two-tailed unpaired student's *t* test.

adipocyte differentiation protocol (Fig. 1*A*). 10T1/2 cells have the potential to differentiate into adipocytes characteristic of brown and beige lineages, exhibiting high levels of thermogenic gene expression and the canonical adrenergic response, i.e., induction of Ppargc1a and Ucp1 gene expression. We analyzed mRNA expression of Ucp1, Cidea, and Ppargc1a in transduced adipocytes following isoproterenol stimulation to screen for putative transcriptional activators of brown and beige adipogenesis.

We obtained a total of 11 positive pools and subsequently identified individual candidate factors in each pool. Heat map representation of gene expression indicates that these factors strongly induced a set of genes responsible for mitochondrial fuel oxidation and thermogenesis (Fig. 1*B*). Among the positive hits are regulators of adipocyte gene expression, including PRDM16, EBF1, E2F1, C/EBPα, and RXRγ. We identified several transcription factors (ZFP91, ZNF787, SP8, GCM2, BATF3, and ZBTB7B) as strong inducers of genes involved in mitochondrial respiration, fatty acid β-oxidation, and uncoupling. Gene-expression analysis indicated that the expression of Zbtb7b was enriched in brown fat (Fig. 1*C*) and significantly increased during brown adipocyte differentiation (Fig. 1 *D* and *E*). We postulated that Zbtb7b may regulate brown and beige adipocyte development and thermogenesis. In support of this, retroviral overexpression of ZBTB7B strongly stimulated the expression of genes involved in fatty acid β-oxidation and mitochondrial oxidative phosphorylation in differentiated 10T1/2 adipocytes (Fig. 1*F*). In addition, ZBTB7B markedly augmented the induction of Ppargc1a and Ucp1 in response to adrenergic stimulation (Fig. 1*G*). The oxygen-consumption study revealed that ZBTB7B significantly increased total respiratory capacity in 10T1/2 adipocytes (Fig. 1*H*). Together, these studies identified Zbtb7b as a transcription factor that activates the thermogenic gene program during adipocyte differentiation.

Zbtb7b Is Required for Brown Fat Development and Thermogenesis. Zbtb7b is a transcription factor that has been demonstrated to regulate $CD4^+$ T-cell development (43–46). However, whether Zbtb7b regulates brown fat development and cold-induced

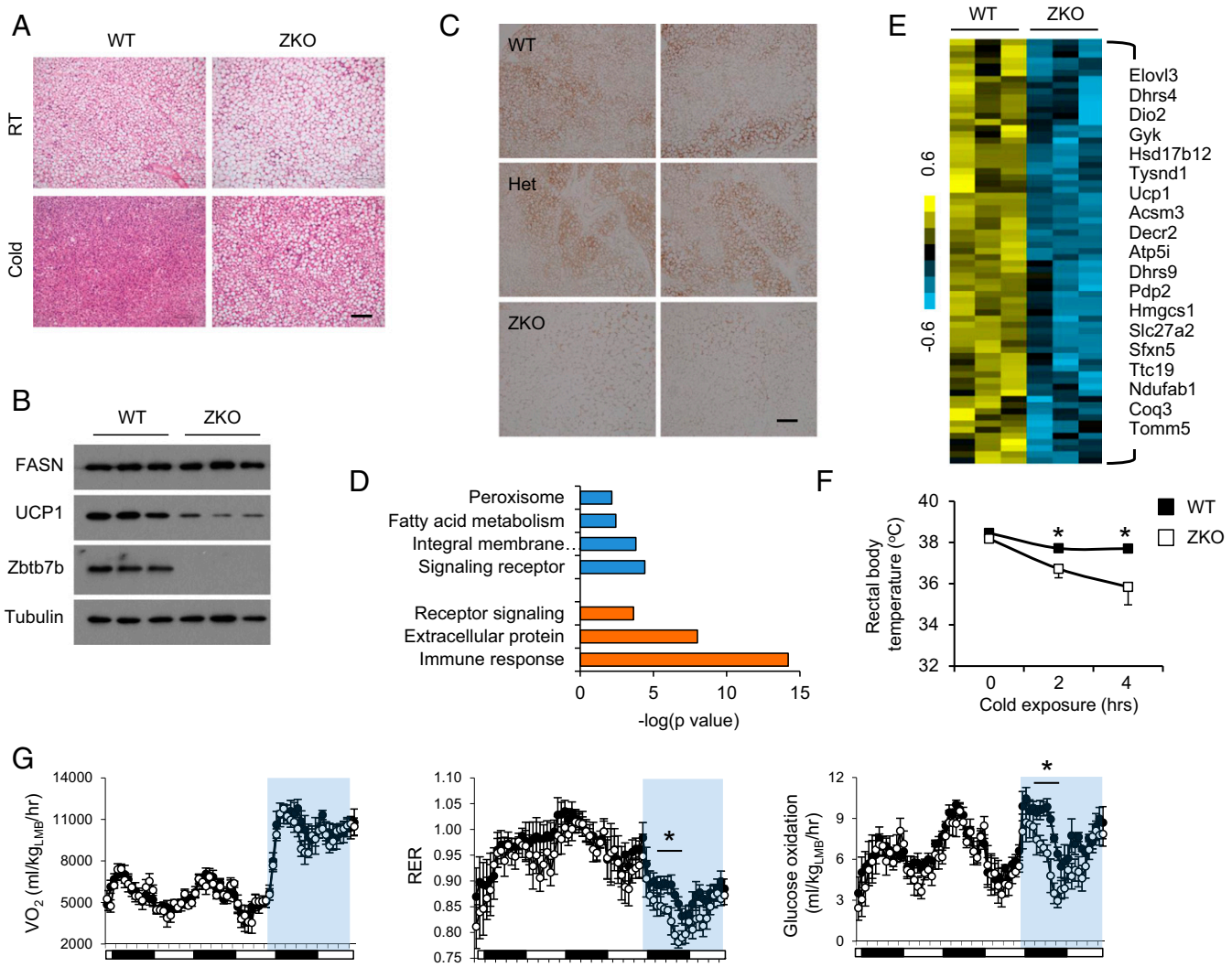

Fig. 2. Zbtb7b is required for thermogenic gene expression in brown fat and defense against cold. (*A*) Histology of brown fat from mice kept at ambient room temperature (RT) or after cold exposure at 4 °C for 4 h. (Scale bar, 100 μm.) (*B*) Immunoblots of brown fat lysates. (*C*) UCP1 immunostaining of brown fat sections from WT, heterozygous (Het), or ZKO mice. (*D*) DAVID pathway analysis for genes down-regulated (blue bars) and up-regulated (red bars) in ZKO brown fat. (*E*) A cluster of genes down-regulated by over 1.6-fold in ZKO brown fat. Genes involved in mitochondrial respiration and thermogenesis are identified on the right. (*F*) Rectal body temperature in WT ($n = 7$, filled squares) and ZKO ($n = 5$, open squares) mice during cold exposure. (*G*) Metabolic cage studies in WT ($n = 5$, filled circles) and ZKO ($n = 5$, open circles) at ambient temperature and 6 °C (light blue). Data represent mean ± SEM. *$P < 0.05$, WT vs. ZKO; two-tailed unpaired student's *t* test.

thermogenesis has not been explored. To determine the significance of Zbtb7b in brown fat thermogenesis, we first examined histological and molecular characteristics of BAT in control WT and Zbtb7b-knockout (ZKO) mice. Compared with control, Zbtb7b-deficient brown adipocytes appeared to have larger lipid droplets at ambient room temperature (Fig. 2*A*), a feature commonly associated with defective brown fat thermogenesis. Immunoblotting and immunohistological staining indicated that UCP1 protein levels were markedly reduced by Zbtb7b deficiency (Fig. 2 *B* and *C*). In contrast, fatty acid synthase (FASN) protein expression remained largely unaltered. Heterozygous deficiency of Zbtb7b appeared to have modest effects on UCP1 expression in brown fat. We next performed microarray transcriptional profiling studies to define how Zbtb7b inactivation alters global gene expression in brown fat. DAVID (Database for Annotation, Visualization and Integrated Discovery) gene ontology analysis indicated that the down-regulated genes are enriched for membrane receptors, fatty acid metabolism, and peroxisome, whereas the up-regulated genes are enriched for immune response, extracellular protein, and receptor signaling (Fig. 2*D*). Among those down-regulated by over 1.6-fold in ZKO mouse brown fat are genes involved in mitochondrial fuel metabolism and thermogenesis (Fig. 2*E*), including Ucp1 and deiodinase 2 (Dio2), an enzyme responsible for local production of thyroid hormone. These observations demonstrate that Zbtb7b is required for maintaining the expression of thermogenic genes in brown fat.

To determine whether these molecular defects impair brown fat thermogenesis, we subjected control and ZKO mice to cold exposure and measured their rectal temperature at different time points. WT mice were able to maintain relatively stable core body temperatures (Fig. 2*F*). In contrast, ZKO mice exhibited cold sensitivity with significantly lower rectal body temperature after 2 h of cold exposure. We next performed metabolic cage studies to assess how Zbtb7b deficiency affects fuel metabolism under normal ambient temperature and cold conditions. As expected, oxygen consumption (VO_2) was markedly increased in WT mice upon switching to cold temperature (Fig. 2*G*). Surprisingly, ZKO mice exhibited a similar increase in VO_2 during cold exposure. Compared with control, the respiratory exchange rate (RER) was significantly lower in ZKO mice following cold switch, which was accompanied by a reduced glucose oxidation rate. As such, Zbtb7b appears to be indispensable for maintaining glucose oxidation during cold-induced thermogenesis, whereas compensatory mechanisms are likely activated to maintain whole-body fuel oxidation.

The above findings raised the possibility that, in addition to its role in maintaining basal brown fat gene expression, Zbtb7b may be indispensable for mediating transcriptional activation of thermogenic genes in response to cold stress. Clustering analysis of the microarray dataset indicated that Zbtb7b deficiency markedly perturbed cold-regulated gene expression in brown fat (Fig. 3*A*). Most notably, a cluster of cold-inducible genes exhibited reduced expression as a result of Zbtb7b inactivation (cluster #1), including Ucp1, Elovl3, and Dio2 (Fig. 3*B*). DAVID analysis indicated that this cluster was moderately enriched for lipid metabolism and Golgi membrane. While mRNA expression of Ebf2 and Ppargc1a was similar between two groups, Blnc1 RNA levels were lower in ZKO brown fat than in control fat under room temperature and cold conditions. The expression of a cluster of cold-repressed genes appeared to be altered by Zbtb7b deficiency following cold exposure (cluster #2). Surprisingly, this cluster was also slightly enriched for genes involved in lipid metabolism, suggesting that Zbtb7b may contribute to cold-induced remodeling of lipid metabolism in brown fat. To establish the cell-autonomous role of Zbtb7b in brown adipocyte development and function, we isolated primary brown preadipocytes from WT and ZKO mice and subjected them to adipogenic induction. In contrast to control, brown adipocytes from ZKO mice failed to mount a normal transcriptional response to adrenergic stimulation. The induction of Ucp1, Elovl3, and Ppargc1a was significantly impaired in Zbtb7b deficiency (Fig. 3*C*). Cidea mRNA levels were markedly lower in ZKO brown adipocytes under basal and stimulated conditions. Together, these results demonstrated that Zbtb7b is critically required for sustaining the expression of the thermogenic gene program in brown fat and defense against cold temperature.

Inactivation of Zbtb7b Impairs Beige Adipocyte Differentiation and White Fat Browning. Despite their distinct development origins, brown and beige adipocytes share a high degree of similarity in the transcriptional control of thermogenic gene expression during differentiation. Our gain-of-function studies in 10T1/2 preadipocytes suggest that Zbtb7b may play an important role in beige adipocyte development. Consistent with this, mRNA expression of Zbtb7b was increased during differentiation of primary beige precursors isolated from inguinal white adipose tissue (iWAT) (Fig. 4*A*). The expression of Blnc1 was also elevated during beige adipogenesis. To clarify the significance of Zbtb7b in beige adipogenesis, we isolated primary iWAT beige precursors from WT and ZKO mice and subjected differentiated adipocytes to treatments with vehicle or isoproterenol. As shown in Fig. 4*B*, adrenergic induction of Ucp1 and Elovl3 expression was markedly reduced in differentiated primary beige adipocytes in the absence of Zbtb7b. Cidea mRNA expression was also reduced under basal and stimulated conditions. These results demonstrate that Zbtb7b is required for the activation of thermogenic genes in beige adipocytes in a cell-autonomous manner.

A prediction of these findings is that in vivo browning of white fat in response to chronic cold exposure may be impaired in ZKO mice. To test this, we subjected WT and ZKO mice to a cold-acclimation protocol, during which housing temperature was gradually decreased to reach 10 °C. After maintaining the mice at 10 °C for 7 d, we harvested adipose tissues and performed gene-expression studies. Consistent with cell culture studies, we found that iWAT from ZKO mice had significantly lower mRNA expression of Ucp1, Cidea, Cox7a1, Dio2, and Gk (Fig. 4*C*). The expression of Cd137, a gene enriched in beige adipocytes, but not Tmem26, was also reduced by Zbtb7b inactivation. The expression of Ucp1, Elovl3, and Gk in brown fat was lower in ZKO mice than in control mice following cold acclimation (Fig. 4*D*). Compared with control, UCP1 protein levels in BAT and iWAT were lower in cold-acclimated ZKO mice (Fig. 4*E*). While H&E histology for iWAT appeared similar, UCP1 immunostaining was also diminished as a result of Zbtb7b deficiency (Fig. 4*F*). While the expression of several transcription factors known to regulate thermogenic adipocyte development, including Ppargc1a, Ebf2, Cebpb, and Prdm16, remained similar, Blnc1 expression was down-regulated in both iWAT and BAT from ZKO mice, suggesting that Blnc1 may be a transcriptional target of Zbtb7b in adipocytes.

Proteomic Analysis of the Adipocyte Zbtb7b Transcriptional Complex. Activation of the thermogenic gene program during brown and beige adipocyte differentiation requires the engagement of a cascade of transcriptional regulators. Zbtb7b deficiency did not alter the expression of Prdm16 and EBF2, suggesting that it may act through mechanisms to regulate the expression of thermogenic genes. To unravel the mechanistic link between Zbtb7b and the transcriptional network governing brown and beige adipogenesis/function, we performed proteomic analysis to identify the components of the Zbtb7b transcriptional complex. We purified the ZBTB7B protein complex from cell lysates prepared from differentiated brown adipocytes expressing vector or Flag/HA-tagged ZBTB7B (FH-ZBTB7B) using a two-step affinity purification protocol. Compared with control, several proteins

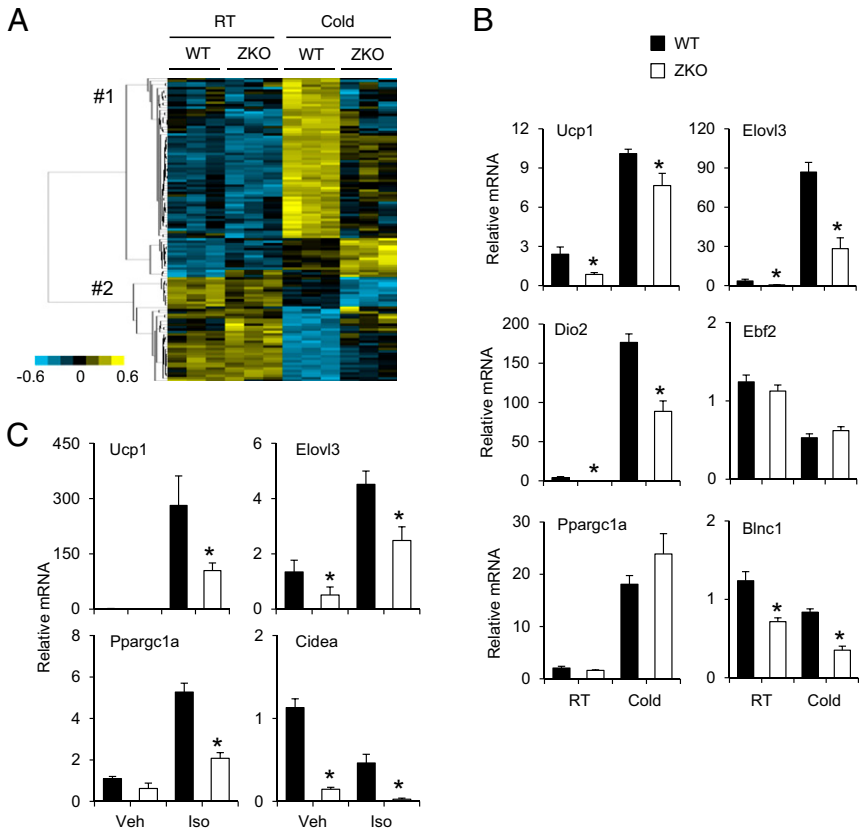

Fig. 3. Zbtb7b orchestrates the transcriptional response of brown adipocytes to cold stress in a cell-autonomous manner. (*A*) Clustering analysis of cold-regulated genes in brown fat from WT and ZKO mice kept at ambient room temperature (RT) or following cold exposure at 4 °C for 4 h. (*B*) qPCR analysis of brown fat gene expression in *A*. Data represent mean ± SEM. $*P < 0.05$, ZKO vs. WT. (*C*) qPCR analysis of gene expression in differentiated primary brown adipocytes treated with vehicle (Veh) or isoproterenol (Iso) for 5 h. Data represent mean ± SD. $*P < 0.05$, ZKO vs. WT; two-tailed unpaired student's *t* test.

were specifically enriched in the ZBTB7B protein complex (Fig. 5*A*). We performed mass spectrometry analysis on the excised bands and identified 13 proteins associated with ZBTB7B, including several RNA-binding proteins, such as hnRNPU, hnRNPM, hnRNPF, hnRNPR, DDX3X, nucleolin (NCL), and Y-box binding protein 1 (YBX1) (Fig. 5*B*). Physical association between ZBTB7B and NEDD4, hnRNPU, NCL, and YBX1 was confirmed by immunoblotting using specific antibodies (Fig. 5*C*). Several factors involved in transcriptional regulation were also present in the ZBTB7B complex, including the linker histone H1 (HIST1H1A, HIST1H1C, and HIST1H1E) and thyroid hormone receptor-associated protein 3 (THRAP3). THRAP3 has been previously implicated in the regulation of adipogenesis through docking on phosphorylated PPARγ (47). To obtain a more comprehensive view of the ZBTB7B transcriptional network, we combined our proteomic data with the protein–protein interaction data for ZBTB7B provided by the human interactome database (Fig. 5*B*). This analysis revealed a protein–protein interaction network of ZBTB7B that may regulate gene transcription through recruiting RNA-binding proteins.

Zbtb7b Recruits the lncRNA Blnc1 Through hnRNPU. Nuclear RNA-binding proteins are important regulators of transcription, pre-mRNA splicing, and RNA processing. We recently identified hnRNPU as a protein that interacts with the lncRNA Blnc1 (41). The physical interaction between ZBTB7B and hnRNPU raised the possibility that hnRNPU may mediate the recruitment of Blnc1 to the ZBTB7B transcriptional complex. We first confirmed the interaction between hnRNPU and ZBTB7B using coimmunoprecipitation in transiently transfected HEK293 cells (Fig. 5*D*). To directly examine the effect of hnRNPU on the recruitment of Blnc1 to ZBTB7B, we performed RNA affinity precipitation using biotin aptamer-tagged Blnc1 (StA-Blnc1) and examined the presence of ZBTB7B in the Blnc1 ribonucleoprotein complex. As shown in Fig. 5*E*, Myc-ZBTB7B was found on the streptavidin beads in the presence of StA-Blnc1 expression; its abundance was further increased by hnRNPU. We performed a reciprocal experiment using immunoprecipitation followed by qPCR (IP/qPCR). Consistently, the association between Blnc1 and ZBTB7B was augmented when hnRNPU was coexpressed in HEK293 cells (Fig. 5*F*). Together, these results demonstrate that hnRNPU facilitates the recruitment of Blnc1 to ZBTB7B.

HnRNPU contains an arginine-glycine-glycine (RGG) RNA-binding domain at the C terminus in addition to other domains, such as the SPRY and SAF domains (48). We transiently transfected HEK293 cells with StA-Blnc1 in the presence of full-length hnRNPU or truncation mutants lacking each of these domains. RNA pulldown analysis indicated that the C-terminal RNA-binding domain is required for its physical interaction with Blnc1 (Fig. 5 *G* and *H*), whereas the SPRY and SAF domains were largely dispensable. The RGG domain appeared to be required for the interaction between hnRNPU and ZBTB7B (Fig. 5*I*). Interestingly, deletion of the SPRY domain strongly increased the recruitment of hnRNPU to ZBTB7B, suggesting that this domain may harbor sequences that negatively regulate the assembly of the Zbtb7b–hnRNPU–Blnc1 transcriptional complex. These molecular studies revealed a mechanism through which Zbtb7b engages the lncRNA regulatory network to control thermogenic gene expression in brown and beige adipocytes.

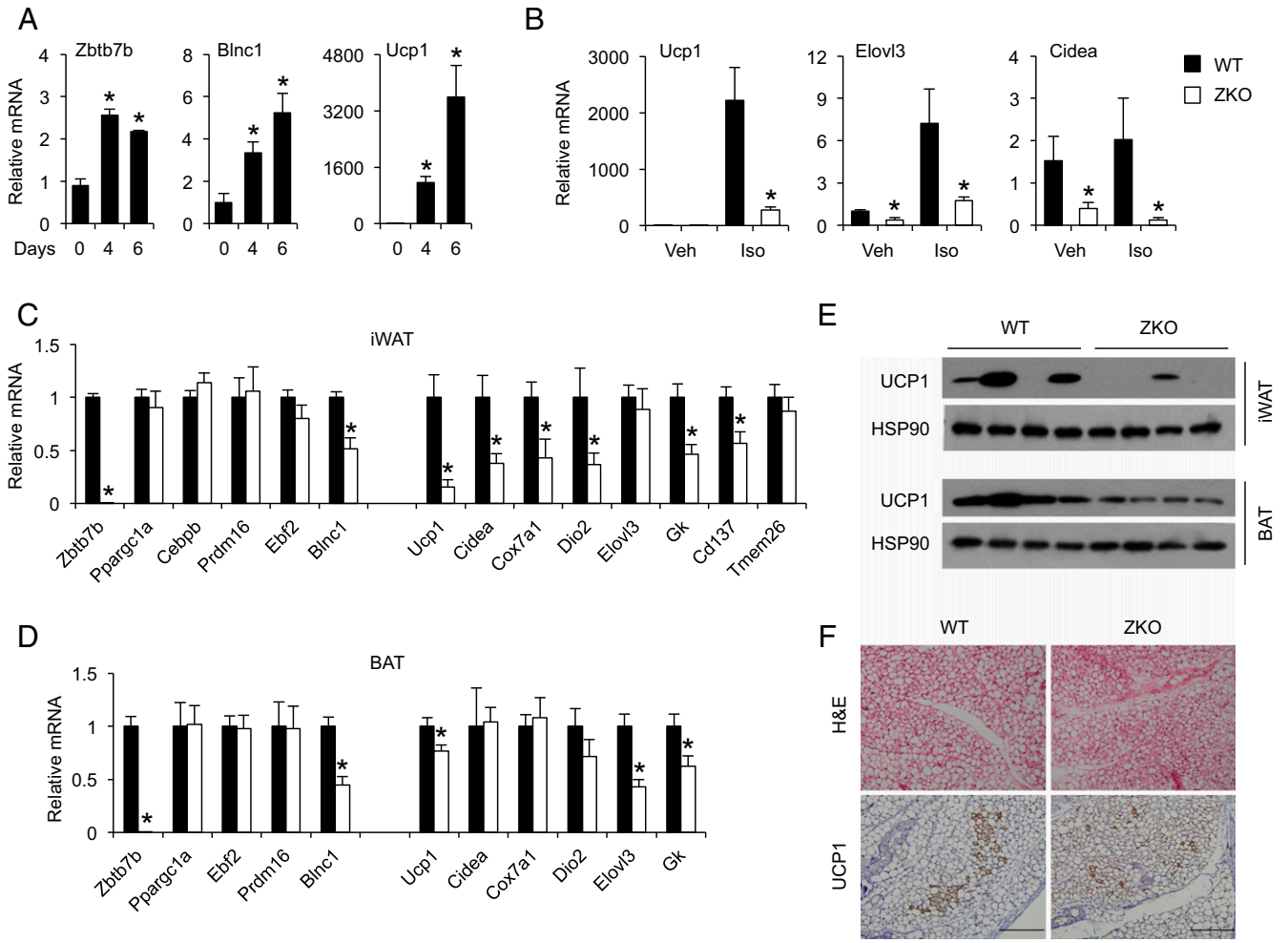

Fig. 4. Inactivation of Zbtb7b impairs beige adipocyte differentiation and inguinal white fat browning. (*A*) qPCR analysis of gene expression during differentiation of preadipocytes isolated from iWAT. Data represent mean ± SD. *$P < 0.01$, vs. d 0; one-way ANOVA. (*B*) qPCR analysis of gene expression in beige adipocytes differentiated from preadipocytes isolated from WT (filled bars) and ZKO (open bars) mice followed by treatments with vehicle (Veh) or isoproterenol (Iso) for 5 h. Data represent mean ± SD. *$P < 0.01$, ZKO vs. WT. (*C* and *D*) qPCR analysis of gene expression in iWAT (*C*) and BAT (*D*) from cold-acclimated WT ($n = 4$, filled bars) and ZKO ($n = 4$, open bars) mice. (*E*) Immunoblots of total BAT and iWAT lysates following cold acclimation. (*F*) H&E and UCP1 immunostaining of iWAT sections. (Scale bars, 200 μm.) Data in *C* and *D* represent mean ± SEM. *$P < 0.05$, ZKO vs. WT; two-tailed unpaired student's *t* test.

Zbtb7b and Blnc1 Form a Feedforward Loop in Thermogenic Gene Induction. We next determined the significance of the hnRNPU/Blnc1 complex in mediating the transcriptional function of ZBTB7B in adipocytes. We used two independent retroviral constructs expressing shRNA against hnRNPU (siU#1 and siU#2) to knock down its expression in brown preadipocytes. RNAi knockdown of hnRNPU significantly impaired the induction of Ucp1 and Cidea expression during brown adipogenesis and reduced mitochondrial DNA content in differentiated adipocytes (Fig. 6 *A* and *B*). To test whether hnRNPU is required for ZBTB7B-induced brown adipogenesis, 10T1/2 preadipocytes transduced with control or siU retroviral vectors in combination with control or ZBTB7B expression vector were subjected to adipogenic differentiation. Differentiated adipocyte cultures were treated with vehicle or isoproterenol before gene-expression analysis. ZBTB7B strongly stimulated mRNA expression of Ucp1, Elovl3, and Cidea in adipocytes expressing control shRNA, particularly following isoproterenol treatments (Fig. 6*C*). In contrast, RNAi knockdown of hnRNPU nearly abolished the stimulatory effects of ZBTB7B in the induction of these thermogenic markers. These results demonstrate that hnRNPU is required for the stimulation of thermogenic gene expression by ZBTB7B through facilitating its recruitment of Blnc1.

As shown above, Zbtb7b deficiency impaired the expression of Blnc1 but not other factors that regulate brown and beige adipogenesis. Consistently, retroviral overexpression of ZBTB7B in brown and 10T1/2 adipocytes significantly increased Blnc1 expression (Fig. 6*D*). A reporter gene assay using the proximal Blnc1 promoter indicated that ZBTB7B strongly stimulated luciferase expression in transient transfection studies (Fig. 6*E*). As such, ZBTB7B may serve as an upstream regulator of Blnc1, providing a feedforward mechanism in driving thermogenic gene expression. In support of this, RNAi knockdown of Blnc1 also significantly impaired the induction of thermogenic gene expression in response to retroviral overexpression of ZBTB7B in 10T1/2 adipocytes (Fig. 6*F*). As shown in Fig. 1, Zbtb7b expression was strongly induced during brown adipocyte differentiation. We next analyzed public ChIP-sequencing (ChIP-seq) datasets to assess whether Zbtb7b is downstream of known adipogenic regulators (49–51). Several robust peaks of chromatin occupancy for EBF2, PPARγ, and PRDM16 were observed in proximity to the Zbtb7b locus (Fig. S1). Retroviral overexpression of PRDM16 strongly stimulated Zbtb7b mRNA expression in brown preadipocytes (Fig. 6*G*), raising the possibility that Zbtb7b may contribute to transcriptional activation of thermogenic genes by PRDM16. Together, these results demonstrate that the recruitment of hnRNPU and Blnc1 serves a

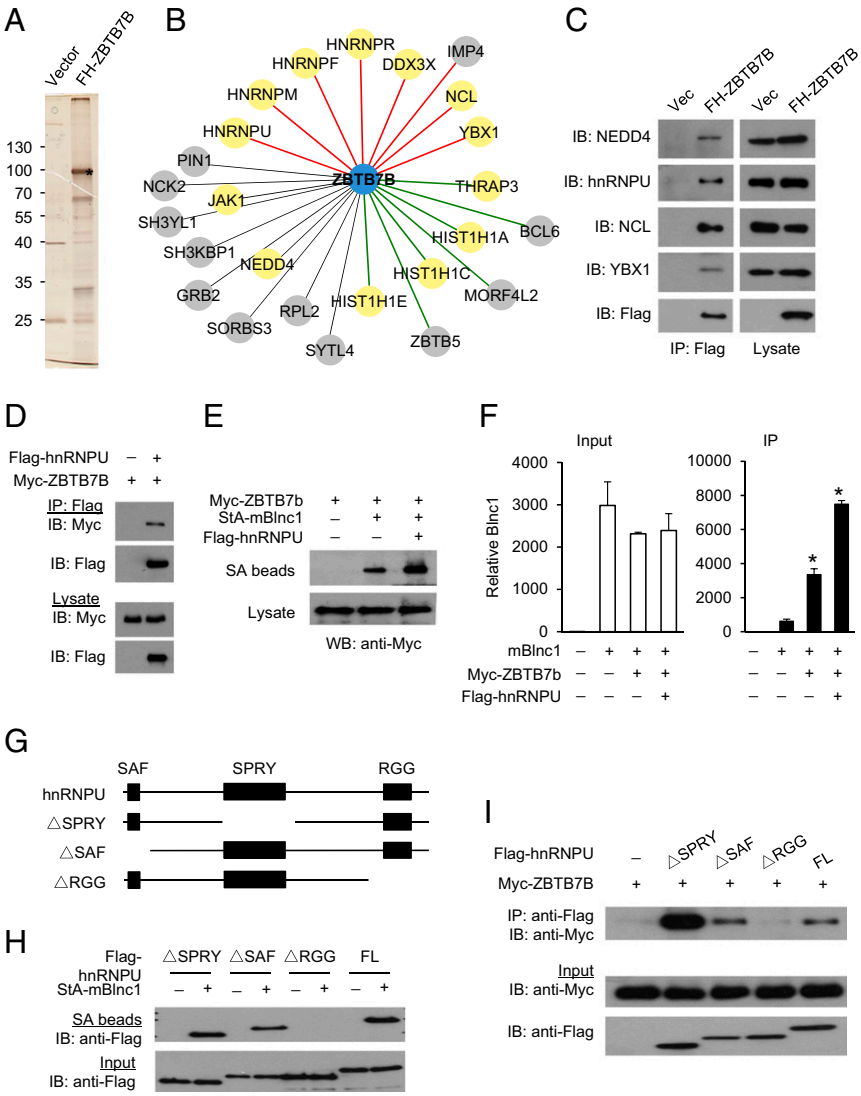

Fig. 5. ZBTB7B recruits the lncRNA Blnc1 through physical interaction with hnRNPU. (*A*) Proteomic analysis of the ZBTB7B protein complex in brown adipocytes. Proteins associated with ZBTB7B were visualized by silver staining following two-step affinity purification. (*B*) A diagram depicting the ZBTB7B interactome based on the current study (yellow circles) and literature (gray circles). Factors involved in RNA binding and processing (red lines), transcriptional regulation (green lines), and signaling (black lines) are indicated. (*C*) Immunoblotting of endogenous proteins associated with FH-ZBTB7B in differentiated brown adipocytes. IB, immunoblot; IP, immunoprecipitation; Vec, vector. (*D*) Coimmunoprecipitation of ZBTB7B and hnRNPU in transiently transfected HEK293 cells. (*E*) Immunoblots of total lysates and precipitated proteins on streptavidin (SA) beads from HEK293 cells transiently transfected with Myc-ZBTB7B and streptavidin aptamer-tagged Blnc1 (StA-Blnc1) in the absence or presence of Flag-hnRNPU. (*F*) qPCR analysis of mBlnc1 in RNA isolated from precipitated immunocomplexes (anti-Myc) (IP) or input from transiently transfected HEK293 cells. Data represent mean ± SD. $^*P < 0.05$, vs. Blnc1 alone; one-way ANOVA. (*G*) A diagram of the hnRNPU truncation mutants. (*H*) Immunoblots of total lysates and precipitated proteins on streptavidin (SA) beads from HEK293 cells transiently transfected with streptavidin aptamer-tagged Blnc1 (StA-Blnc1) plus hnRNPU mutants. (*I*) Immunoblots of total lysates and anti-Flag immunoprecipitated proteins from HEK293 cells transiently transfected with Myc-ZBTB7B and Flag-hnRNPU (FL) plasmids.

critical role in mediating transcriptional activation of thermogenic gene expression in adipocytes.

Discussion

The interface between protein factors and lncRNAs in biological control remains poorly understood. Using a genome-wide functional screen, we identified Zbtb7b as a transcriptional factor that promotes brown fat development and thermogenesis. Zbtb7b is required for differentiation of brown and beige adipocytes in culture and cold-induced beige fat formation in inguinal white fat. At the mechanistic level, Zbtb7b recruits the hnRNPU/Blnc1 ribonucleoprotein complex to stimulate the expression of genes involved in fuel oxidation and thermogenesis (Fig. 6*H*). Interestingly, Blnc1 itself is a downstream target of Zbtb7b, which thereby act together in a feedforward manner. Zbtb7b and EBF2 therefore represent two key regulatory nodes that interface with lncRNA regulators to control adipocyte development and metabolism.

Several lines of evidence support an important role of Zbtb7b in brown and beige fat development. First, retroviral overexpression of Zbtb7b strongly stimulated the expression of key thermogenic markers in 10T1/2 and brown adipocytes, including Ucp1, Cidea, and Ppargc1a. Genetic inactivation of Zbtb7b impaired the differentiation of primary brown and beige adipocytes in culture. Consistently, brown adipocytes in Zbtb7b-null mice exhibited increased lipid accumulation with a concomitant impairment of thermogenic gene expression. Zbtb7b appears to be dispensable for the specification of brown adipocyte lineage, as

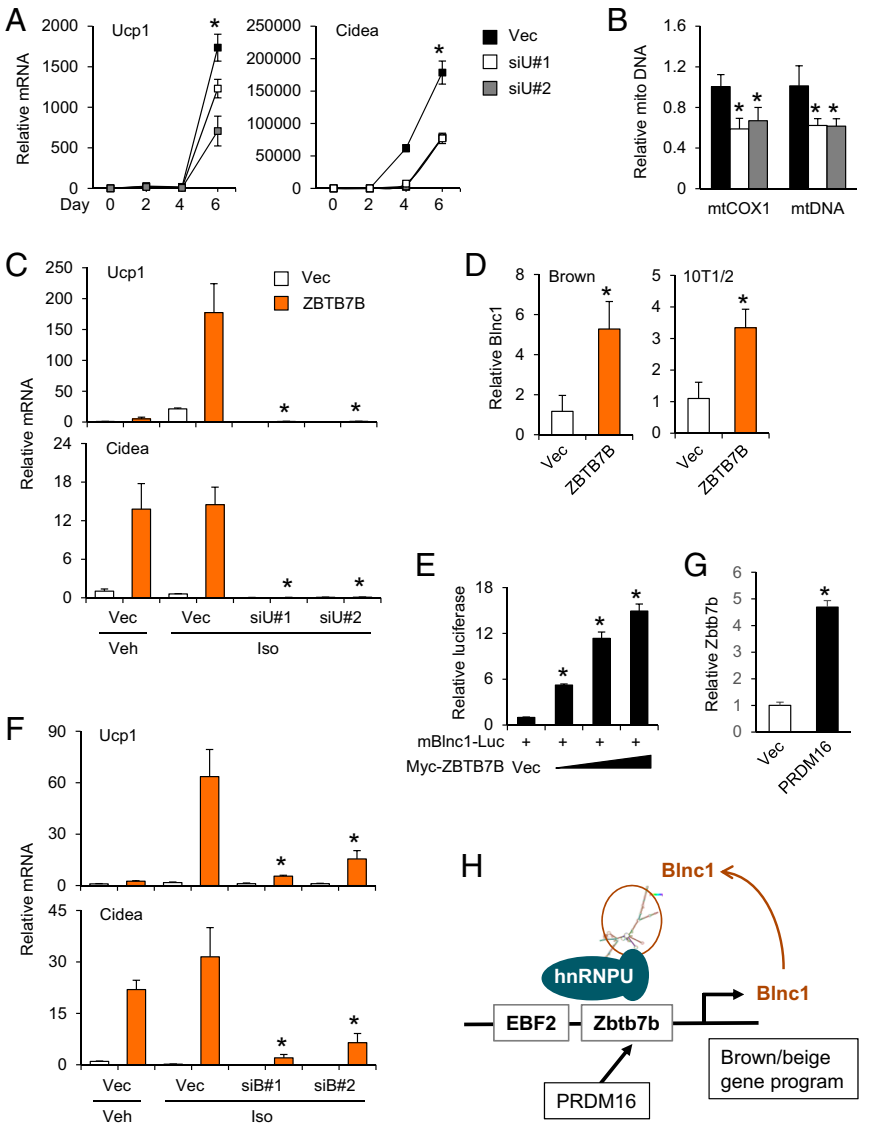

Fig. 6. A Zbtb7b–Blnc1 feedforward regulatory loop in thermogenic gene induction. (*A*) qPCR analyses of gene expression in control (Vec) and hnRNPU-knockdown (siU#1 and #2) 10T1/2 adipocytes at different time points. (*B*) Mitochondrial DNA content in differentiated 10T1/2 adipocytes. Data in *A* and *B* represent mean ± SD. *$P < 0.05$ vs. Vec; two-tailed unpaired Student's *t* test. (*C*) Control and hnRNPU-knockdown10T1/2 preadipocytes were transduced with vector (open bars) or ZBTB7B (red bars) retrovirus. Differentiated adipocytes were treated with vehicle (Veh) or isoproterenol (Iso) for 5 h. Data represent mean ± SD. *$P < 0.05$, vs. Vec; two-tailed unpaired student's *t* test. (*D*) qPCR analysis of Blnc1 expression in differentiated brown (*Left*) and 10T1/2 (*Right*) adipocytes. Data represent mean ± SD. *$P < 0.05$, vs. vehicle; two-tailed unpaired student's *t* test. (*E*) Reporter gene assay. Data represent mean ± SD. *$P < 0.01$, Myc-ZBTB7B vs. Vec; one-way ANOVA. (*F*) qPCR analyses of gene expression. 10T1/2 preadipocytes were transduced with control (open bars) or ZBTB7B (red bars) retroviruses in combination with control (Vec) or shRNA retroviral vectors targeting Blnc1 (siB#1 and siB#2). Differentiated adipocytes were treated with vehicle (Veh) or isoproterenol (Iso) for 5 h. Data represent mean ± SD. *$P < 0.05$, siB#1 and #2 vs. Vec; two-tailed unpaired student's *t* test. (*G*) qPCR analysis of Zbtb7b mRNA expression in brown preadipocytes transduced with vector (Vec) or PRDM16 retrovirus. Data represent mean ± SD. *$P < 0.01$, vs. Vec. (*H*) A model depicting activation of the thermogenic gene program in brown/beige adipocytes through a feedforward loop between lncRNA and transcription factors.

the formation of brown fat depot was largely unaffected in ZKO mice. These observations suggest that Zbtb7b likely acts at stages after progenitor commitment, i.e., during adipocyte differentiation and maturation. Zbtb7b-null mice failed to fully activate the transcriptional program associated with cold-induced thermogenesis and were unable to mount an effective thermogenic response during cold exposure. In the context of chronic cold exposure, Zbtb7b deficiency impaired beige fat induction in the s.c. fat, indicating that this factor regulates a transcriptional program common to brown and beige adipocytes.

An intriguing mechanistic aspect of the regulation of thermogenic gene expression by Zbtb7b is its recruitment of the Blnc1/hnRNPU ribonucleoprotein transcriptional complex. Our proteomic studies revealed that Zbtb7b physically associates with a number of RNA-binding proteins, including several hnRNPs, DDX3X, NCL, and YBX1. Interestingly, YBX1 has been previously identified as an interacting protein for EWS, another RNA-binding protein, in the regulation of brown fat development (52). These observations raise the possibility that Zbtb7b may engage the lncRNA regulators through its association with RNA-binding proteins. In support of this, hnRNPU facilitates the recruitment of Blnc1 to Zbtb7b in RNA–protein interaction assays. The RGG RNA-binding motif on hnRNPU is indispensable for this activity. The critical role of hnRNPU and Blnc1 in mediating the transcriptional function of Zbtb7b is illustrated by RNAi-knockdown studies. shRNA-mediated

depletion of hnRNPU and Blnc1 markedly impaired the stimulatory effects of Zbtb7b on thermogenic gene expression in adipocytes. Previous studies demonstrated that hnRNPU physically interacts with lnc-BATE1 (37). It remains possible that Zbtb7b may recruit multiple lncRNAs in thermogenic adipocytes through its physical interaction with RNA-binding proteins.

Our functional screen revealed a much broader set of transcription factors and cofactors that regulate adipocyte thermogenic gene expression. Several factors known to regulate adipocyte gene expression scored positive in our screen, including PRDM16, EBF1, CEBPA, E2F1, and RXRG, underscoring the success of this screen in identifying relevant regulators of adipocyte development and metabolism. In addition to Zbtb7b, we also identified several other candidates; however, their role in adipocyte differentiation and thermogenesis remains to be characterized, particularly in loss-of-function settings. With the discovery of an increasing number of transcription factors and lncRNAs that regulate adipogenesis, a major challenge is to delineate how these factors are integrated to control the diverse aspects of adipocyte biology. Future studies on the interface between protein and RNA regulators are expected to reveal unprecedented details of the mechanisms underlying the genetic control of adipocyte development and metabolism.

Methods

Transcription Factor Screen. Generation of the TFORC was described previously (42). The current TFORC version includes a total of 1,510 transcription factors and cofactors after adding 364 ORFs not included in the original collection. These ORF inserts were cloned into a murine stem cell virus (MSCV) retroviral destination vector containing an N-terminal Flag-HA tag using LR recombinase. Four individual TFORC clones were pooled for retroviral production and the initial screen. C3H10T1/2 cells were obtained from ATCC and maintained in DMEM containing 10% FBS. The fibroblasts were plated on 12-well plates 1 d before retroviral transduction in medium containing 4 μg/mL Polybrene in the presence of 200 μL of the retroviral suspension. To increase transduction efficiency, culture plates were spun at 18 × *g* for 30 min and then incubated overnight before changing to fresh culture medium. After reaching confluence, the cells were split into two 12-well plates, subjected to adipocyte differentiation, and analyzed by qPCR for gene expression and Oil Red O staining for lipid accumulation.

Adipocyte Differentiation. Primary brown adipocytes were immortalized and induced to differentiate as previously described (39, 41). For 10T1/2 adipocyte differentiation, confluent cultures were exposed to induction medium containing DMEM supplemented with 10% FBS containing 0.5 μM isobutylmethylxanthine (IBMX), 125 μM indomethacin, 1 μM dexamethasone, 1 nM triiodothyronine (T3), and 20 nM insulin (Sigma Aldrich). After 48 h, the induction medium was replaced with maintenance medium (DMEM supplemented with 10% FBS, 1 nM T3, and 20 nM insulin). Fresh maintenance medium was added every 2 d until day 7. For Oil Red O staining, adipocytes were fixed in 2% formaldehyde for 10 min and stained for 60 min with 0.2% Oil Red O followed by washing in double-distilled H_2O.

Mice. All animal care and experimental procedures were approved by the University of Michigan Committee on Use and Care of Animals. The generation of Zbtb7b-knockout mice, in which exons 2 and 3 of Zbtb7b were deleted, resulting in a null allele, was previously described (43). We obtained ZKO mice in the C57BL/6 background from the Jackson Laboratory and maintained the colony by breeding between heterozygous mice. Mice were fed ad libitum and maintained under 12/12-h light/dark cycles. For cold exposure, 10-wk-old mice were individually housed in cages prechilled at 4 °C with free access to food and water. Core body temperature was monitored using a rectal thermometer at indicated time points. For cold acclimation, mice were transferred into a temperature-controlled chamber. The temperature in the chamber was lowered 3 °C every day until it reached 10 °C. Mice were then maintained at 10 °C for 7 d before being killed. Tissues were dissected and immediately frozen in liquid nitrogen before RNA and protein analyses.

Primary Cell Culture. Primary cell isolation and differentiation from inguinal white fat and interscapular BAT were described previously (53). Briefly, fat tissues were removed from 8- to 10-wk-old mice and minced before digestion in Collagenase D and Dispase II for 20 min in a 37 °C water bath shaker. The digested tissues were then filtered through a 100-μm cell strainer to remove tissue debris and mature adipocytes. The stromal vascular fraction (SVF) was pelleted by centrifugation, resuspended, and filtered through a 40-μm strainer before plating onto collagen-coated dishes. The culture was maintained in DMEM/F12 GlutaMAX (Thermo Fisher) supplemented with 15% FBS. The primary progenitor culture was passed no more than three times before plating onto 12-well plates for differentiation. To induce differentiation, confluent cells were incubated with induction medium (DMEM/F12 GlutaMAX containing 10% FBS, 0.5 μg/mL insulin, 2 μM dexamethasone, 1 μM rosiglitazone, and 0.5 mM IBMX). Two (iWAT) or three (BAT) days later, the medium was replaced with maintenance medium (DMEM/F12 GlutaMAX supplemented with 10% FBS and 0.5 μg/mL insulin) for a total of 7–8 d when adipocytes were fully differentiated.

Gene-Expression Analyses. Total RNA from differentiated adipocytes was extracted using the TRIzol method following the manufacturer's instructions. Total tissue RNA was isolated using the PureLink RNA isolation kit (Thermo Fisher). For RT-qPCR, 2 μg of RNA was reverse-transcribed using Moloney Murine Leukemia Virus (MMLV)-RT followed by qPCR using SYBR Green (Life Technologies). Relative mRNA expression was normalized to the ribosomal protein 36B4.

Histology and Immunohistochemistry. For histology, adipose tissues were dissected and fixed in 10% formalin overnight at 4 °C before paraffin embedding and H&E staining. For immunohistochemistry, unstained tissue sections were heated at 60 °C for 30 min before rehydration. Antigen retrieval was achieved by boiling the slides in 10 mM sodium citrate-citric acid solution (pH 6.2) for 20 min. Endogenous peroxidase activity was blocked by submerging the slides in 3% H_2O_2 prepared in methanol for 15 min. The slides were incubated with blocking reagent (5% BSA, 0.5% Tween-20, 0.05% NaN3 in PBS) for 30 min followed by the addition of anti-Ucp1 antibody at 4 °C overnight. The slides were washed three times with PBST (0.5% Tween 20 in PBS) and incubated with ImmPRESS (peroxidase) polymer anti-Rabbit IgG reagent for 1 h followed by exposure to HRP substrate 3,3-diaminobenzidine (DAB) (Vector Laboratory). The slides were subsequently dehydrated by dipping sequentially through 70%, 95%, 100% ethanol and xylene before mounting (Permount; Thermo Fisher).

Mass Spectrometry Analysis of the ZBTB7B Protein Complex. The Zbtb7b protein complex was purified using the method described previously (54, 55). Briefly, total lysates were prepared from brown adipocytes stably expressing vector or Flag-HA-ZBTB7B and subjected to affinity purification using anti-Flag (Sigma) affinity matrix. Bound protein complexes were eluted by excess Flag peptide and underwent a second affinity step using anti-HA agarose (Roche). Protein eluted by HA peptide was analyzed on SDS/PAGE followed by silver staining. Bands were excised for mass spectrometry analysis to identify the proteins. Additional interacting proteins for ZBTB7B were obtained from the human interactome database (interactome.dfci.harvard.edu).

Immunoblotting Analysis. Total cell lysates were prepared in a lysis buffer containing 50 mM Tris·HCl (pH 7.8), 137 mM NaCl, 10 mM NaF, 1 mM EDTA, 1% Triton X-100, 10% glycerol, and the protease inhibitor mixture (Roche) after three freeze/thaw cycles. Tissue lysates were prepared by homogenizing in a buffer containing 50 mM Tris (pH 7.6), 130 mM NaCl, 5 mM NaF, 25 mM β-glycerophosphate, 1 mM sodium orthovanadate, 10% glycerol, 1% Triton X-100, 1 mM DTT, 1 mM PMSF, and the protease inhibitor mixture. The antibodies used were rabbit anti-FASN (3180S; Cell Signaling), rabbit anti-UCP1 (UCP11-A; Alpha Diagnostic), mouse anti-Zbtb7b (sc-376250; Santa Cruz), rabbit anti-Hsp90 (sc-7947; Santa Cruz), mouse anti-Flag (F1804; Sigma), mouse anti-hnRNPU (sc-32315; Santa Cruz), mouse anti-Myc (M5546; Sigma), rabbit anti-Myc (C3956; Sigma), mouse anti-tubulin (T6199; Sigma), rabbit anti-NEDD4 (21698-1-AP; Proteintech), rabbit anti-YBX1 (9744S; Cell Signaling Technology), and rabbit anti-nucleolin (14574S; Cell Signaling Technology).

Reporter Gene Assays. The Blnc1 luciferase reporter was constructed by cloning the proximal promoter of Blnc1 1.5 kb into the pGL3 Basic vector (Promega). The luciferase assay was performed in HEK293 cells, as previously described (54). Briefly, 100 ng of mBlnc1 reporter plasmid was mixed with vector or with 100, 200, or 400 ng of ZBTB7B expression constructs. Equal amounts of DNA were used for all wells by supplementing appropriate amounts of vector plasmid. Relative luciferase activities were determined 48 h following transfection. All transfection experiments were performed in triplicates.

RNA–Protein Interaction Assays. HEK293 cells cultured on six-well plates were transiently transfected with Flag-hnRNPU, Myc-ZBTB7B, and StA-Blnc1 alone or in combinations. For anti-SA agarose beads, total lysates were prepared in a lysis buffer that contained 20 mM Tris (pH 7.5), 100 mM KCl, 5 mM $MgCl_2$, 1% Nonidet P-40, and freshly added protease inhibitors and RNase inhibitor (S1402S; New England Biolabs). The lysates were immunoprecipitated using streptavidin agarose beads for 90 min at 4 °C, followed by washing three times with wash buffer [50 mM Tris (pH 7.5), 150 mM NaCl, 1 mM $MgCl_2$, 0.5% Nonidet P-40]. For anti-Flag and anti-Myc agarose beads, total lysates were prepared in a lysis buffer that contained 50 mM Tris·HCl (pH 7.8), 137 mM NaCl, 1 mM EDTA, 1% Triton X-100, 10% glycerol, and fresh protease inhibitors. The lysates were immunoprecipitated using anti-Flag or anti-Myc agarose beads for 2 h at 4 °C, followed by washing three times with wash buffer [20 mM Tris (pH 8.0), 0.2 mM EDTA, 100 mM KCl, 2 mM MgCl2, 0.1% Tween 20, 10% glycerol]. For IP/qPCR, RNA remaining on the affinity beads was extracted using TRIzol, treated with RNase-free DNase, and analyzed by qPCR. For RNA pull-down, total lysates were extracted with SDS and analyzed by immunoblotting.

ACKNOWLEDGMENTS. We thank Dr. Shinichi Nakagawa (RIKEN) for providing the hnRNPU truncation constructs; Xiaoling Peng for technical support; and James Delproposto in the Center for Structural Biology at the University of Michigan for assistance with robotics for high-throughput plasmid purification. This work was supported by NIH Grant DK102456 (to J.D.L.), American Diabetes Association Grant 1-15-BS-118 (to J.D.L.), and Pilot Grant P30DK089503 from the Michigan Nutrition Obesity Research Center (to S.L.). L.M. was supported by Predoctoral Fellowship 201506300141 from the Chinese Scholarship Council. X.Y.Z. was supported by NIH Pathway to Independence Award DK106664.

1. Kajimura S, Saito M (2014) A new era in brown adipose tissue biology: Molecular control of brown fat development and energy homeostasis. *Annu Rev Physiol* 76: 225–249.
2. Cannon B, Nedergaard J (2004) Brown adipose tissue: Function and physiological significance. *Physiol Rev* 84:277–359.
3. Harms M, Seale P (2013) Brown and beige fat: Development, function and therapeutic potential. *Nat Med* 19:1252–1263.
4. Townsend KL, Tseng YH (2014) Brown fat fuel utilization and thermogenesis. *Trends Endocrinol Metab* 25:168–177.
5. Wu J, Cohen P, Spiegelman BM (2013) Adaptive thermogenesis in adipocytes: Is beige the new brown? *Genes Dev* 27:234–250.
6. Lowell BB, et al. (1993) Development of obesity in transgenic mice after genetic ablation of brown adipose tissue. *Nature* 366:740–742.
7. Bartelt A, et al. (2011) Brown adipose tissue activity controls triglyceride clearance. *Nat Med* 17:200–205.
8. Hanssen MJ, et al. (2015) Short-term cold acclimation improves insulin sensitivity in patients with type 2 diabetes mellitus. *Nat Med* 21:863–865.
9. van der Lans AA, et al. (2013) Cold acclimation recruits human brown fat and increases nonshivering thermogenesis. *J Clin Invest* 123:3395–3403.
10. Yoneshiro T, et al. (2013) Recruited brown adipose tissue as an antiobesity agent in humans. *J Clin Invest* 123:3404–3408.
11. Villarroya F, Cereijo R, Villarroya J, Giralt M (2017) Brown adipose tissue as a secretory organ. *Nat Rev Endocrinol* 13:26–35.
12. Wang GX, Zhao XY, Lin JD (2015) The brown fat secretome: Metabolic functions beyond thermogenesis. *Trends Endocrinol Metab* 26:231–237.
13. Wang GX, et al. (2014) The brown fat-enriched secreted factor Nrg4 preserves metabolic homeostasis through attenuation of hepatic lipogenesis. *Nat Med* 20: 1436–1443.
14. Nedergaard J, Cannon B (2010) The changed metabolic world with human brown adipose tissue: Therapeutic visions. *Cell Metab* 11:268–272.
15. Tseng YH, Cypess AM, Kahn CR (2010) Cellular bioenergetics as a target for obesity therapy. *Nat Rev Drug Discov* 9:465–482.
16. Cypess AM, et al. (2009) Identification and importance of brown adipose tissue in adult humans. *N Engl J Med* 360:1509–1517.
17. Nedergaard J, Bengtsson T, Cannon B (2007) Unexpected evidence for active brown adipose tissue in adult humans. *Am J Physiol Endocrinol Metab* 293:E444–E452.
18. van Marken Lichtenbelt WD, et al. (2009) Cold-activated brown adipose tissue in healthy men. *N Engl J Med* 360:1500–1508.
19. Virtanen KA, et al. (2009) Functional brown adipose tissue in healthy adults. *N Engl J Med* 360:1518–1525.
20. Seale P, et al. (2008) PRDM16 controls a brown fat/skeletal muscle switch. *Nature* 454: 961–967.
21. Berry DC, Jiang Y, Graff JM (2016) Mouse strains to study cold-inducible beige progenitors and beige adipocyte formation and function. *Nat Commun* 7:10184.
22. Long JZ, et al. (2014) A smooth muscle-like origin for beige adipocytes. *Cell Metab* 19: 810–820.
23. Min SY, et al. (2016) Human 'brite/beige' adipocytes develop from capillary networks, and their implantation improves metabolic homeostasis in mice. *Nat Med* 22:312–318.
24. Inagaki T, Sakai J, Kajimura S (2016) Transcriptional and epigenetic control of brown and beige adipose cell fate and function. *Nat Rev Mol Cell Biol* 17:480–495.
25. Cohen P, et al. (2014) Ablation of PRDM16 and beige adipose causes metabolic dysfunction and a subcutaneous to visceral fat switch. *Cell* 156:304–316.
26. Harms MJ, et al. (2014) Prdm16 is required for the maintenance of brown adipocyte identity and function in adult mice. *Cell Metab* 19:593–604.
27. Dempersmier J, et al. (2015) Cold-inducible Zfp516 activates UCP1 transcription to promote browning of white fat and development of brown fat. *Mol Cell* 57:235–246.
28. Kong X, et al. (2014) IRF4 is a key thermogenic transcriptional partner of PGC-1α. *Cell* 158:69–83.
29. Ohno H, Shinoda K, Ohyama K, Sharp LZ, Kajimura S (2013) EHMT1 controls brown adipose cell fate and thermogenesis through the PRDM16 complex. *Nature* 504: 163–167.
30. Seale P, et al. (2007) Transcriptional control of brown fat determination by PRDM16. *Cell Metab* 6:38–54.
31. Rinn JL, Chang HY (2012) Genome regulation by long noncoding RNAs. *Annu Rev Biochem* 81:145–166.
32. Atkinson SR, Marguerat S, Bähler J (2012) Exploring long non-coding RNAs through sequencing. *Semin Cell Dev Biol* 23:200–205.
33. Li P, et al. (2015) A liver-enriched long non-coding RNA, lncLSTR, regulates systemic lipid metabolism in mice. *Cell Metab* 21:455–467.
34. Sallam T, et al. (2016) Feedback modulation of cholesterol metabolism by the lipid-responsive non-coding RNA LeXis. *Nature* 534:124–128.
35. Arnes L, Akerman I, Balderes DA, Ferrer J, Sussel L (2016) βlinc1 encodes a long noncoding RNA that regulates islet β-cell formation and function. *Genes Dev* 30: 502–507.
36. Morán I, et al. (2012) Human β cell transcriptome analysis uncovers lncRNAs that are tissue-specific, dynamically regulated, and abnormally expressed in type 2 diabetes. *Cell Metab* 16:435–448.
37. Alvarez-Dominguez JR, et al. (2015) De novo reconstruction of adipose tissue transcriptomes reveals long non-coding RNA regulators of brown adipocyte development. *Cell Metab* 21:764–776.
38. Sun L, et al. (2013) Long noncoding RNAs regulate adipogenesis. *Proc Natl Acad Sci USA* 110:3387–3392.
39. Zhao XY, Li S, Wang GX, Yu Q, Lin JD (2014) A long noncoding RNA transcriptional regulatory circuit drives thermogenic adipocyte differentiation. *Mol Cell* 55:372–382.
40. Zhao XY, Lin JD (2015) Long noncoding RNAs: A new regulatory code in metabolic control. *Trends Biochem Sci* 40:586–596.
41. Mi L, Zhao XY, Li S, Yang G, Lin JD (2016) Conserved function of the long noncoding RNA Blnc1 in brown adipocyte differentiation. *Mol Metab* 6:101–110.
42. Li S, et al. (2008) Genome-wide coactivation analysis of PGC-1alpha identifies BAF60a as a regulator of hepatic lipid metabolism. *Cell Metab* 8:105–117.
43. Egawa T, Littman DR (2008) ThPOK acts late in specification of the helper T cell lineage and suppresses Runx-mediated commitment to the cytotoxic T cell lineage. *Nat Immunol* 9:1131–1139.
44. He X, et al. (2008) CD4-CD8 lineage commitment is regulated by a silencer element at the ThPOK transcription-factor locus. *Immunity* 28:346–358.
45. Muroi S, et al. (2008) Cascading suppression of transcriptional silencers by ThPOK seals helper T cell fate. *Nat Immunol* 9:1113–1121.
46. Wang L, et al. (2008) Distinct functions for the transcription factors GATA-3 and ThPOK during intrathymic differentiation of CD4(+) T cells. *Nat Immunol* 9: 1122–1130.
47. Choi JH, et al. (2014) Thrap3 docks on phosphoserine 273 of PPARγ and controls diabetic gene programming. *Genes Dev* 28:2361–2369.
48. Chen H, et al. (2010) Mitochondrial fusion is required for mtDNA stability in skeletal muscle and tolerance of mtDNA mutations. *Cell* 141:280–289.
49. Harms MJ, et al. (2015) PRDM16 binds MED1 and controls chromatin architecture to determine a brown fat transcriptional program. *Genes Dev* 29:298–307.
50. Shapira SN, et al. (2017) EBF2 transcriptionally regulates brown adipogenesis via the histone reader DPF3 and the BAF chromatin remodeling complex. *Genes Dev* 31: 660–673.
51. Soccio RE, et al. (2015) Genetic variation determines PPARγ function and anti-diabetic drug response in vivo. *Cell* 162:33–44.
52. Park JH, et al. (2013) A multifunctional protein, EWS, is essential for early brown fat lineage determination. *Dev Cell* 26:393–404.
53. Wu J, et al. (2012) Beige adipocytes are a distinct type of thermogenic fat cell in mouse and human. *Cell* 150:366–376.
54. Hernandez C, Molusky M, Li Y, Li S, Lin JD (2010) Regulation of hepatic ApoC3 expression by PGC-1β mediates hypolipidemic effect of nicotinic acid. *Cell Metab* 12: 411–419.
55. Wang GX, et al. (2014) Otopetrin 1 protects mice from obesity-associated metabolic dysfunction through attenuating adipose tissue inflammation. *Diabetes* 63: 1340–1352.